$Ru_3(CO)_{12}$ in Acidic Media. Intermediates of the Acid-Cocatalyzed Water-Gas Shift Reaction (WGSR)

Giuseppe Fachinetti,* Tiziana Funaioli,* Lorenzo Lecci, and Fabio Marchetti

Dipartimento di Chimica e Chimica Industriale, Università di Pisa, via Risorgimento 35, I-56126 Pisa, Italy

Received May 28, 1996[⊗]

The elucidation of the WGSR promoted by ruthenium carbonyls in acidic media started with the detection of the Ru(0), Ru(I), and Ru(II) intermediate complexes, namely $Ru_3(CO)_{12}$, $Ru_2[\mu\text{-}\eta^2\text{-}OC(CF_3)O]_2(CO)_6$, and *fac*-$[Ru(CF_3COO)_3(CO)_3]^-$, which accumulate when CF_3COOH is employed as an acid cocatalyst. Under catalytic conditions, the three were found to interconvert through elementary steps which produce CO_2 and H_2. In fact, Ru(0) is oxidized by H^+ to Ru(I) and half the hydrogen of the catalytic cycle is supplied by this reaction. On the other hand, Ru(I) disproportionates to Ru(0) and Ru(II), and this latter species undergoes nucleophilic attack by H_2O. The decomposition of the metallacarboxylic acid intermediate gives back Ru(I), while H_2 and CO_2 are produced in a 1/2 molar ratio. The two alternating pathways for dihydrogen formation, namely Ru(0) oxidation by H^+ and the decomposition of a metallacarboxylic acid intermediate, involve H_2 reductive elimination from the same $RuHCF_3COO(CO)_2L_2$ intermediate (L = H_2O, ethers). These findings define an acid-cocatalyzed WGSR whose distinctive features are (i) the intervention of a disproportionation reaction to generate a Ru(II) electron poor complex, whose CO ligands can undergo nucleophilic attack by water, (ii) the generation of the hydrido intermediate for dihydrogen production through two distinct reaction patways, and (iii) the reductive elimination of H_2 from the hydrido intermediate without involving H^+ from the medium.

Introduction

In acidic media $Ru_3(CO)_{12}$ is a catalyst precursor for homogeneous WGSR,[1] for the addition of carboxylic acids to alkynes,[2] and, under conditions of high temperature and pressure, for the production of ethylene glycol derivatives from syngas[3] and for the syngas homologation of CH_3OH,[4] esters,[5] and carboxylic acids.[6] On the other hand, the known fundamental chemistry of ruthenium carbonyls in acidic solutions is unsufficient for the complete understanding of these catalytic reactions: all are believed to involve hydrido intermediates whose origin and nature were not demonstrated, however. Moreover, in the case of the here disclosed acid-cocatalyzed WGSR, not only the nature of the dihydrogen yielding hydrido complex but also the origin and the nature of the mandatory intermediates,[7] bearing CO ligands susceptible of attack by water in acidic solutions, still remained obscure. On trying to characterize them, we met with some new aspects of the chemistry of ruthenium carbonyls, which are fundamental for a better understanding of catalytic reactions.

Experimental Section

General Methods. Unless otherwise specified, all operations were carried out under argon by standard Schlenk techniques. CO (<0.1% H_2) was purchased from Matheson, and AR grade toluene, py, iso-PrOH, THF, THF-d_8, diglyme, CF_3COOH, CF_3COOCs, CF_3SO_3H, and $NaBPh_4$ from Aldrich. The ethers were further purified by distilling them from $LiAlH_4$, with THF and THF-d_8 under an Ar atmosphere and diglyme under vacuum; CF_3COOCs was anhydrified under vacuum at 120 °C. Ruthenium trichloride hydrate was used as received from Chimet SpA. The ruthenium complex $Ru_3(CO)_{12}$ was prepared by literature methods.[8] The IR spectra were recorded on a Perkin-Elmer Model FT-IR 1725-X, and ^1H and ^{19}F NMR spectra on a Varian Model Gemini-200. Liquid samples for infrared spectra were taken off with a syringe and transferred to a 0.1 mm CaF_2 cell. Analyses of H_2 in gas samples from catalysis run were performed by a DANI Model 3200 gas chromatograph equipped with HW detector and a molecular sieve column with Ar as carrier gas. A calibration curve was prepared periodically. CO_2 was determined by bubbling the reaction gases through 25 mL aliquots of a 0.098 N $Ba(OH)_2$ solution and back-titration (phenolphthalein end point) of $Ba(OH)_2$ excess. The apparatus and procedures for the gas volumetric measurements were those described in the literature.[9]

Batch Reactor Procedures. Catalytic activity runs were carried out at 95 °C, P_{CO} = 0.8 atm in an all glass vessel with a volume of 316 mL, similar to that described in the literature.[10] During a typical run, gas samples (1 mL) were removed at 1.5-h intervals and analyzed by GC.

$Ru_2[\mu\text{-}\eta^2\text{-}OC(CF_3)O]_2(CO)_6$ (1a). $Ru_3(CO)_{12}$ (5.0 g, 7.82 mmol) was suspended in diglyme containing 8 M H_2O and 0.8 M CF_3COOH (total volume = 100 mL) and heated to 100 °C during 12 h. The resulting orange solution was concentrated under vacuum (20 mmHg, 100 °C) leaving a deep red oil which was treated with toluene (200 mL). This homogeneous solution was stirred under CO atmosphere at 40 °C during 2 h and then stored 24 h at −20 °C. A 5.9 g amount of pale yellow crystals of **1a** (85% yield) was obtained and gave satisfactory analytical data. FT-IR (Nujol mull): ν_{CO} 2102 vs, 2051 vs, 2017 vs, 1993 s, and 1665 s cm^{-1}.[11]

$Ru_2[\mu\text{-}\eta^2\text{-}OC(CF_3)O]_2(CO)_4L_2$ (L = H_2O, Diglyme) (1b). A 0.350 g amount of **1a** was dissolved in diglyme containing 8 M H_2O (total

[⊗] Abstract published in *Advance ACS Abstracts,* November 1, 1996.

(1) Yarrow, P.; Cohen, H.; Ungermann, C.; Vanerberg, D.; Ford, P. C.; Rinker, R. G. *J. Mol. Catal.* **1983,** *22*, 239.
(2) Rothem, M.; Shvo, Y. *J. Organomet. Chem.* **1993**, *448*, 189.
(3) Dombek, B. D. *Adv. Catal.* **1983**, *32*, 325.
(4) Braca, G.; Sbrana, G.; Valentini, G.; Andrich, G.; Gregorio, G. *J. Am. Chem. Soc.* **1978,** *100*, 6238.
(5) Braca, G.; Sbrana, G.; Gregorio, G. U.S. Patent 4,189,441, **1980**.
(6) (a) Knifton, J. F. *J. Mol. Catal.* **1981**, *11*, 91. (b) Knifton, J. F. *Chem. Techn.* **1981,** 609. (c) Knifton, J. F. *Hydr. Proc.* **1981**, *60*, 113.
(7) Collman, J. P.; Hegedus, L. S.; Norton, J. R.; Finke, R. G. *Princples and Applications of Organotransition Metal Chemistry*; University Science Book: Mill Valley, CA, 1987.
(8) Braca, G.; Sbrana, G.; Pino, P. *Chim. Ind.* (*Milan*) **1964**, *46*, 206; *Chim. Ind.* (*Milan*) **1968**, *50*, 121.
(9) Calderazzo, F.; Cotton, F. A. *Inorg. Chem.* **1962**, *1*, 30.
(10) Pardey, A. J.; Ford, P. C. *J. Mol. Catal.* **1989**, *53*, 247.
(11) Rotem, M.; Goldberg, I; Shmueli, U; Shvo, Y. *J. Organomet. Chem.* **1986**, *314*, 185.

S0020-1669(96)00630-1 CCC: $12.00 © 1996 American Chemical Society

Table 1. Crystal Data and Details of Structure Refinements

empirical formula	$C_9CsF_9O_9Ru$	$C_{10}H_8F_6O_8Ru$	$C_{41}H_{36}BN_3O_2Ru$
fw	657.07	471.23	714.61
temp, K	293(2)	293(2)	293(2)
wavelength, Å	0.71073	0.71073	1.54178
cryst system	monoclinic	monoclinic	hexagonal
space group	$P2_1/c$ (No. 14)	$P2_1/c$ (No. 14)	$P6_5$ (No. 170)
a, Å	8.3839(5)	12.486(2)	9.7604(6)
b, Å	14.450(3)	10.228(2)	9.7604(9)
c, Å	16.079(1)	12.286(2)	64.244(8)
α, deg	90	90	90
β, deg	102.951(5)	107.76(2)	90
γ, deg	90	90	120
V, Å^3	1898.4(4)	1494.2(5)	5300.3(9)
Z	4	4	6
D(calc), Mg/m^3	2.299	2.095	1.343
abs coeff, mm^{-1}	2.840	1.159	3.892
F(000)	1224	920	2208
cryst size, mm	0.34 × 0.24 × 0.22	0.25 × 0.25 × 0.08	0.21 × 0.21 × 0.48
θ range for data collcn, deg	1.92−24.99	2.63−20.99	5.23−59.85
h ranges	−1 to 9	−12 to 12	−8 to 0
k ranges	−1 to 17	−10 to 1	0 to 10
l ranges	−19 to 18	−1 to 12	−72 to 64
reflcns collcd	4312	2134	5129
indepdt reflcns	3248 [$R_{int} = 0.022$]	1596 [$R_{int} = 0.057$]	5129
refinement method	full-matrix least squares on F^2	full-matrix least squares on F^2	full-matrix least squares on F^2
data/restraints/params	3240/30/239	1596/16/150	5129/5/436
goodness-of-fit on F^2	1.029	1.069	1.108
final *R* indices [$I > 2\sigma(I)$]	$R_1 = 0.0526$, $wR_2 = 0.1278$	$R_1 = 0.0890$, $wR_2 = 0.2200$	$R_1 = 0.0343$, $wR_2 = 0.0764$
R indices (all data)	$R_1 = 0.0727$, $wR_2 = 0.1863$	$R_1 = 0.1633$, $wR_2 = 0.2865$	$R_1 = 0.0735$, $wR_2 = 0.0886$
largest diff peak and hole, e·Å^{-3}	1.110 and −0.794	1.212 and −0.981	0.841 and −1.178

volume = 20 mL), and the solution was briefly evacuated. Under an inert atmosphere the IR spectrum consisted of the absorptions of **1b** at 2043 s, 1989 m, and 1958 vs cm^{-1}.[11] By restoration of a CO atmosphere, gas absorption took place and absorptions of **1a**, together with those of **1b** became evident.

[*fac*-Ru(OCOCF$_3$)$_3$(CO)$_3$]Cs (2). A catalytic run was carried out by employing $Ru_3(CO)_{12}$ (0.250 g, 0.39 mmol) in diglyme containing 8 M H_2O, 3 M CF_3COOH, and 0.4 M CF_3COOCs (total volume = 20 mL). The run was protracted overnight and then stopped by lowering the temperature to 20 °C. Colorless crystals of **2** (0.310 g, 40% yield), suitable for an X-ray investigation, separated out within 1 day. Satisfactory analytical data were obtained. FT-IR (Nujol mull): ν_{CO} 2145 s, 2084 vs 2067 vs, and 1693 s cm^{-1}. The molecular structure is reported in Figure 2.

Disproportionation Reaction of 1a. 1a (0.650 g, 1.09 mmol) and CF_3COOCs (0.270 g, 1.09 mmol) were dissolved in 20 mL of anhydrous THF and placed under a CO atmosphere at 30 °C. Within 8 h, 1.07 mmol of gas was absorbed while orange $Ru_3(CO)_{12}$ separated out (0.220 g, 0.34 mmol, 95% yield; ν_{CO} (*n*-hexane) 2061 s, 2031 s, and 2013 m cm^{-1}). On evaporation of the mother liquor to dryness under vacuum, a pale yellow residue of **2** was obtained (0.710 g, 1.08 mmol, 99% yield; ν_{CO} (Nujol): 2145 s, 2084 vs, 2067 vs, and 1693 s cm^{-1}).

Reaction between 2 and H_2O. (a) At 95 °C, in the Presence of CF_3COOH. A 20 mL aliquot of a 8 M H_2O, 0.5 M CF_3COOH, and 0.036 M **2** (0.470 g, 0.71 mmol) solution in diglyme was placed under an Ar atmosphere in the 316 mL reaction vessel used for the catalytic runs. By the increase of the temperature up to 95 °C, the colorless solution turns yellow. After 1 hour the H_2 (0.35 mmol, 99% yield) and the CO_2 (0.69 mmol, 97% yield) were quantitatively determined. The IR spectrum of the liquid phase showed only the absorptions of **1b.** ν_{CO}: 2043 s, 1989 m, 1958 s cm^{-1}.

(b) At Room Temperature. 2 (0.443 g, 0.67 mmol) was dissolved in diglyme containing 8 M H_2O (total volume = 20 mL) under an Ar atmosphere in the 316 mL reaction vessel used for the catalytic runs. A pale yellow color was immediately observed, and the reaction was monitored by IR spectroscopy. After 45 min at room temperature, only the IR absorptions of a **3a**−**c** mixture of hydrido complexes became detectable (ν_{CO}: 2041 and 1957 cm^{-1}). Only trace amounts of H_2 were detected in the gas phase, while quantitative determination of the produced CO_2 gave 0.62 mmol (92% yield).

Dihydrogen Formation from a 3a−c Mixture of Hydrides. 4 (0.470 g, 1 mmol) was reacted at room temperature with 8 M H_2O in diglyme (total volume = 20 mL) in the vessel for catalytic runs. After 45 min CO_2 formation ceased; the atmosphere was replaced by pure argon and the temperature raised to 65 °C. Gas samples (1 mL) were periodically taken off, and H_2 was determined by GC (Figure 6). After 24 h the IR spectrum of the liquid phase showed only the absorptions of **1b** (ν_{CO}: 2043 s, 1989 m, 1958 s cm^{-1}). An identical solution ([Ru] = 0.05 M, [H_2O] = 8 M in diglyme, total volume = 20 mL) in the same 316 mL reaction vessel was treated with 130 μL (1.5 mmol) of CF_3SO_3H at the end of CO_2 formation and then warmed to 65 °C. The H_2 formed at various times was determined as before.

{*fac*-Ru(OCOCF$_3$)$_2$(CO)$_3$[(CH$_3$)$_2$CHOH]} (4). $Ru_3(CO)_{12}$ (5.0 g, 7.82 mmol) was suspended in diglyme containing 8 M H_2O and 2.2 M CF_3COOH (total volume = 50 mL) and warmed to 100 °C during 12 h. The resulting orange solution of **1a** was stirred under a $P_{CO} = 1$ atm at room temperature for 5 days. As a consequence of the disproportionation reaction, $Ru_3(CO)_{12}$ separated out and was removed by filtration. The mother liquor was evaporated to dryness under vacuum at 100 °C, leaving an orange oil which was dissolved in 15 mL of *iso*-PrOH. A 200 mL volume of toluene was then added and the solution concentrated under vacuum at room temperature, till the precipitation of colorless crystals of **4** occurred (3.43 g, 7.28 mmol, 31% yield; ν_{CO} (Nujol) 2153 s, 2094 vs, 2078 vs, and 1676 s, broad, cm^{-1}). Satisfactory analytical data were obtained. The molecular structure is shown in Figure 3.

^{1}H NMR Spectra. 2 (0.130 g, 0.20 mmol) was dissolved in THF-d_8 containing 8 M H_2O (total volume 0.5 mL) and allowed to stand for 1 h. The spectrum of Figure 4a was then obtained. **4** (0.095 g, 0.20 mmol) was dissolved in THF-d_8 containing 8 M H_2O (total volume 0.5 mL) and allowed to stand for 1 h. The spectrum of Figure 4b was obtained and was converted into that of Figure 4a by addition of 0.052 g (0.21 mmol) of solid CF_3COOCs, directly in the NMR tube. In another experiment **4** was reacted with 8 M H_2O in THF-d_8 at the same concentration as before. By means of a syringe, increasing amounts of CF_3SO_3H were then added directly into the NMR tube. The spectra of Figure 4c−f were obtained at CF_3SO_3H/Ru = 0.42, 0.72, 1.36, and 2.40 molar ratios, respectively.

[*fac*-RuH(CO)$_2$(py)$_3$][BPh$_4$] (5). 4 (1.32 g, 2.8 mmol) was dissolved in 25 mL of THF, and 5 mL of H_2O was added at room temperature. After 1 h, 1.3 g (3.8 mmol) of $NaBPh_4$ in 20 mL of py was added, and the product was precipitated by addition of 150 mL of CH_3OH. After 1 week at 4 °C 1.7 g (2.38 mmol, 85% yield) of **5**[17] was collected as colorless crystals. The molecular structure is reported in Figure 5.

X-ray Structure Determinations. The crystals of [*fac*-Ru(OCOCF$_3$)$_3$(CO)$_3$]Cs are colorless monoclinic prisms defined by the form {011} closed by the pinacoid {100}. One of them was glued at the end of a glass fiber and was mounted on a Siemens P4 automatic single-crystal diffractometer, equipped with a graphite-monochromatized Mo Kα radiation. Cell parameters were calculated on the accurately centered setting angles of 25 strong reflections with $12.5° \leq \theta \leq 13°$. Details about the crystal parameters and intensity data collection are summarized in the second column of Table 1. The Laue class was established by an automatic procedure contained in the diffractometer control program.[12] A redundant set of data was collected to estimate the collection accuracy. Three standard reflections measured every 97 measurements showed no decay in the crystal. The space group was univocally established as $P2_1/c$ on the basis of systematic absences. The collected intensities were corrected for Lorentz and polarization effects and for absorption by a Gaussian integration method.[13] The equivalent reflections present in the set were then merged resulting in an internal R value ($R_{int} = \sum|F_o^2 - F_o^2(\text{mean})|/\sum(F_o^2)$) of 0.022. The structure was solved by the automatic Patterson method contained in the SHELXTL[2] program, and the molecule was completed by means of the next Fourier map. Disorder in the positions of the CF_3 groups was suggested by electron density maps. The disorder was explained as a statistical distribution of the trifluoroacetate groups on two different conformations, and two different CF_3 groups were introduced in each position imposing the sums of occupancies equal to 1.

The final refinement cycles were made with anisotropic thermal factors for Cs, Ru, O, and C atoms and isotropic for F atoms and imposing geometrical constraints to the CF_3 modifications. The final reliability factors are showed in Table 1, where $R_1 = \sum||F_o| - |F_c||/\sum|F_o|$, $wR_2 = [w(F_o^2 - F_c^2)^2/w(F_o^2)^2]^{1/2}$, and $w = 1/[\sigma^2(F_o^2) + (0.0636P)^2 + 12.34P]$, with $P = [\max(F_o^2,0) + 2Fc^2]/3$ and $S = [w(F_o^2 - F_c^2)^2/(N - P)]^{1/2}$.

The crystals of {*fac*-Ru(OCOCF$_3$)$_2$(CO)$_3$[(CH$_3$)$_2$CHOH]} (**4**) are colorless milky, with a prismatic shape. Some of them were sealed within glass capillaries under a nitrogen atmosphere and were examined on a Siemens P4 single-crystal diffractometer. All the samples appeared to be crystalline, but not one presented a good diffraction profile. In fact some profiles appeared to be exceedingly large and some other showed a depression in the central part of the profile as they corresponded to two different single crystals slightly misaligned. The third column of Table 1 summarizes the relevant crystal data and intensity data collection details. Cell parameters were calculated from the setting angles of 13 accurately centered strong reflections having $8.9° \leq \theta \leq 9.6°$. The choice of such a low value for max, here and in the intensities collection, has been called for by the lack of intense diffractions at high angles.

A redundant set of data was collected to verify, on merging, the collection reliability. Three standard reflections measured every 97 measurements allowed one to exclude any crystal decay. The collected data were corrected for Lorentz and polarization effects, but not for absorption, since a scanning around the ψ angle of 5 intense reflections showed a slight effect on the measured intensity.

The space group was univocally established as $P2_1/c$ by systematic extinctions, and the structure was solved by direct methods contained in the TREF[13] procedure. However, the two CF_3 groups of the trifluoroacetate ligands and two methyl groups of isopropyl alcohol could not be reliably localized in a rather smeared electron density that appeared on the Fourier map. We explained this fact with the presence of disorder both in $-CF_3$ and in $-CH(CH_3)_2$ groups. As in the case of the cesium salt, we have introduced two distinct idealized $-CF_3$ groups in each expected position of trifluoroacetate ligand and two different $-CH(CH_3)_2$ groups in the isopropyl alcohol, assuming a total occupancy equal to 1 for each group. The atoms found in the Fourier map were refined with anisotropic thermal factors, while isotropic factors have been used for the disordered atoms that have been introduced in geometrically calculated positions and have been refined as rigid groups. The hydrogen atoms were not introduced.

The final reliability parameters are shown in Table 1, where R_1, wR_2, and S have the same meaning as in the preceeding column and $w = 1/[\sigma^2(F_o^2) + (0.1454P)^2 + 15.38P]$, where $P = [\max(F_o^2,0) + 2F_c^2]/3$. The reliability appears acceptable considering the poor quality of the crystal and the presence of disorder.

The crystals of [RuH(CO)$_2$(py)$_3$][BPh$_4$] are colorless hexagonal prisms closed by hexagonal bipyramids. One of them was glued at the end of a glass fiber, and its diffraction pattern was studied on a Weissenberg camera using Cu Kα radiation ($\lambda = 1.541\,78$ Å). The pattern showed well-shaped spots displaying hexagonal symmetry and a very long c period. The systematic extinctions suggested a primitive lattice with a 6_1 or 6_5 operator.

Accurate cell parameters and intensity data were collected on a Nonius CAD4 single-crystal diffractometer equipped with graphite-monochromatized Cu Kα radiation. Crystal parameters and collection details are summarized in the fourth column of Table 1. Collection of three standard reflections every 97 measurements allowed one to exclude any crystal decay. The collected data were corrected for Lorentz and polarization effects and for absorption by using a ψ-scan method. The structure was solved by standard Patterson and Fourier methods in the $P6_5$ space group, and the absolute configuration of the crystal was chosen on the basis of Flack index.[14] The hydrogen atoms were introduced in calculated positions and were allowed to ride on the connected carbon atoms. The final reliability indexes obtained in the last least-squares cycles, with all the heavy atoms with anisotropic thermal parameters, are shown in the last column of Table 1, where $w = 1/[\sigma^2(F_o^2) + (0.0427P)^2 + 0.09P]$ with $P = [\max(F_o^2,0) + 2F_c^2]/3$.

All calculations and drawings were performed by using the SHELXTL[13] program.

Results and Discussion

Direct Detection of Intermediates during the CF_3COOH-Cocatalyzed WGSR. We recently evidenced that the nature of conjugated base affects the acid-cocatalyzed WGSR promoted by $Rh_4(CO)_{12}$.[15] A role of the conjugated base is apparent also in the case, examined here, of the $Ru_3(CO)_{12}$ precursor in H_2O/diglyme solution: by comparison of two strong acids, *i.e.* sulfuric and triflic, as cocatalysts for the WGSR under the same conditions, only the former resulted in activity. Moreover, by the employment of CF_3COOH as cocatalyst in the 8 M H_2O/diglyme medium ([Ru] = 0.036 M, [CF_3COOH] = 0.5 M, P_{CO} = 0.8 atm, T = 95 °C) the TOF(H_2) (TOF(H_2) = mol of H_2/mol of Ru/day) was 3 and increased to 18 on adding CF_3COOCs in a 1/5 molar ratio with respect to the acid. Such a sharp increase of TOF(H_2) demonstrates the beneficial role of CF_3COO^- and can be understood by considering that CF_3COOH behaves as a weak acid in the reaction medium ($\kappa_a = 2 \times 10^{-2}$ at 25 °C).[16] Therefore, the addition of CF_3COOCs, although only in a 1/5 molar ratio with respect to the acid, strongly increases the concentration of its conjugated base.

Remarkably, the CF_3COO^- concentration also affects the nature of the intermediate carbonyl complexes which accumulate during WGSR. At the low CF_3COO^- concentration arising from the dissociation of CF_3COOH, only dimeric Ru(I) carbonyls, namely a P_{CO}-depending equilibrium mixture of $Ru_2[\mu\text{-}\eta^2\text{-}OC(CF_3)O]_2(CO)_6$ (**1a**) and $Ru_2[\mu\text{-}\eta^2\text{-}OC(CF_3)O]_2(CO)_4L_2$ (L = H_2O, diglyme) (**1b**),[11] can be detected by IR analysis after the early stages of catalysis (Figure 1a). When the CF_3COO^- concentration is substantially increased by the addition of CF_3COOCs, however, two new absorptions (ν_{CO} 2136 and 2065

(12) XSCANS: *X-ray Single Crystal Analysis System*, rel. 2.1; Siemens Analytical X-ray Instruments Inc.: Madison, WI, 1994.
(13) Sheldrick, G. M. *SHELXTL-Plus, Rel. 5.03*; Siemens Analytical X-ray Instruments Inc.: Madison, WI, 1994.
(14) Flack, H. D. *Acta Crystallogr.* **1983**, *A39*, 876.
(15) Fachinetti, G.; Fochi, G.; Funaioli, T. *Inorg. Chem.* **1994**, *33*, 1719.
(16) This value was determined by fitting the ^{19}F NMR chemical shift data of progressively diluted CF_3COOH solutions (5×10^{-1} to 5×10^{-4} M, 25 °C) in diglyme containing 8 M H_2O, to equation which describes the dependence of the concentration C_o on the measured chemical shift (Dimicoli, J. L.; Helene, C. J. *J. Chem. Soc.* **1973**, *95*, 1036), affords the value of 2×10^{-2}.

cm^{-1}; Figure 1b) point out the accumulation of a new electrophilic carbonyl.

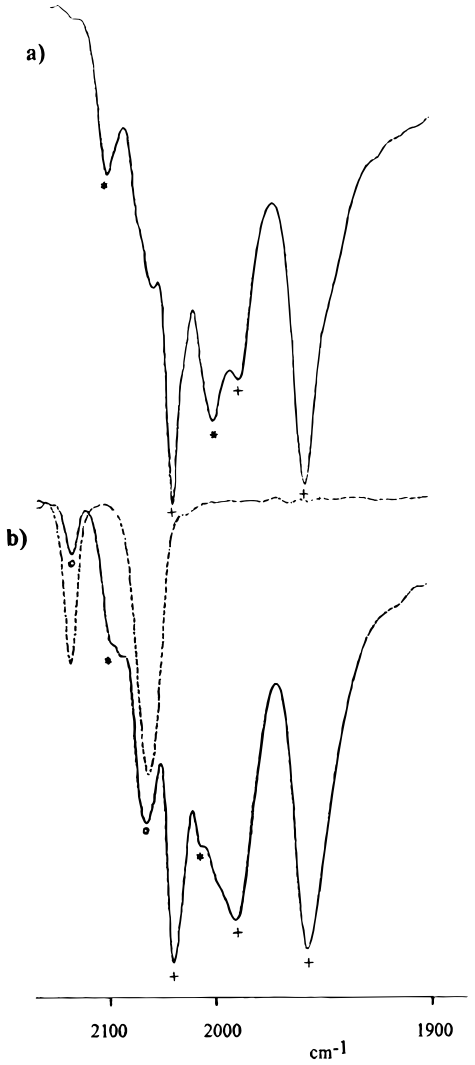

Figure 1. (a) IR spectrum in the CO stretching region of samples withdrawn during the WGSR in diglyme containing 8 M H_2O ([Ru] = 0.036 M, [CF_3COOH] = 0.5 M, P_{CO} = 0.8 atm, T = 95 °C). (b) IR spectrum in CO stretching region of samples withdrawn during the WGSR at increased [CF_3COO^-] by addition of CF_3COOCs in a 1/5 molar ratio with respect to CF_3COOH. For a comparison, the spectrum of 0.015 M **2** in diglyme containing 8 M H_2O and 0.5 M CF_3COOH has been inserted (dashed line). The absorptions of the H_2O/CF_3COOH/diglyme medium have been subtracted. Key: (*) absorptions of **1a**; (+) absorptions of (**1b**); (○) absorptions of **2**.

In order to characterize this latter species, WGSR was carried out in a more concentrated solution at 95 °C. On cooling of the sample to room temperature, a colorless precipitate, suitable for a single-crystal X-ray analysis, separated out. The IR spectra of this product in the solid state (ν_{CO} 2145 s, 2084 vs, and 2067 vs, cm^{-1}) and in an acidic H_2O/diglime solution (Figure 1b, dashed line) confirm that it is the same carbonyl complex which is found to accumulate when the homogeneous catalysis is carried out in the presence of excess CF_3COO^-. The molecular structure shows that it is the cesium salt of [*fac*-Ru$(OCOCF_3)_3(CO)_3]^-$ (**2**) (Figure 2); the main bond distances and angles are summarized in Table 2.

Reactions Interconverting the Intermediates and Producing CO_2 and H_2. The formation of the equilibrium mixture of **1a**,**b**, the only products found to accumulate at low CF_3COO^- concentration (eq 1), parallels a number of well-known reactions

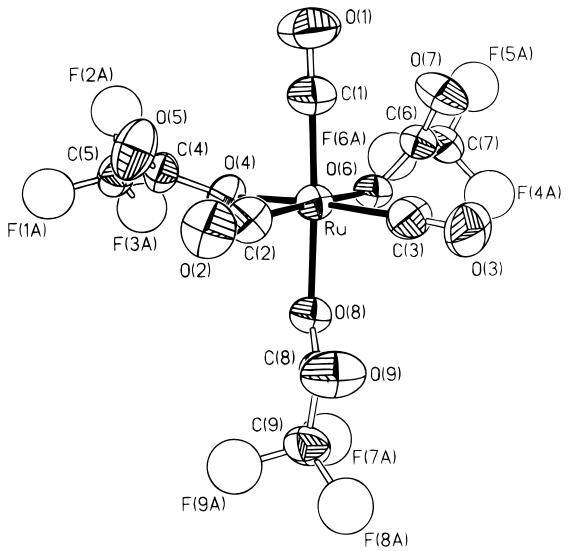

Figure 2. ORTEP projection of the structure of the anionic moiety of [*fac*-Ru$(OCOCF_3)_3(CO)_3$]Cs (**2**). Ru, C, and O atoms are represented by thermal ellipsoids at 50% probability. The disordered F atoms have been refined with isotropic thermal displacement factors and are here represented by spheres. For clarity, only one of the two limit positions of the fluorine atoms is shown.

Table 2. Bond Lengths (Å) and Angles (deg) for the Anion [*fac*-Ru$(OCOCF_3)_3(CO)_3]^-$

Ru−C(1)	1.896(10)	O(4)−C(4)	1.267(10)
Ru−C(2)	1.914(10)	O(5)−C(4)	1.198(11)
Ru−C(3)	1.925(10)	C(4)−C(5)	1.520(11)
Ru−O(8)	2.088(6)	O(6)−C(6)	1.269(10)
Ru−O(4)	2.091(6)	O(7)−C(6)	1.213(11)
Ru−O(6)	2.096(6)	C(6)−C(7)	1.552(12)
C(1)−O(1)	1.142(11)	O(8)−C(8)	1.280(10)
C(2)−O(2)	1.130(11)	O(9)−C(8)	1.194(11)
C(3)−O(3)	1.107(11)	C(8)−C(9)	1.543(12)
C(1)−Ru−C(2)	89.5(4)	O(1)−C(1)−Ru	177.1(10)
C(1)−Ru−C(3)	92.8(4)	O(2)−C(2)−Ru	177.4(9)
C(2)−Ru−C(3)	90.2(4)	O(3)−C(3)−Ru	178.2(8)
C(1)−Ru−O(8)	174.1(3)	C(4)−O(4)−Ru	122.7(6)
C(2)−Ru−O(8)	93.2(3)	O(5)−C(4)−O(4)	129.1(9)
C(3)−Ru−O(8)	92.5(3)	O(5)−C(4)−C(5)	119.6(8)
C(1)−Ru−O(4)	92.8(4)	O(4)−C(4)−C(5)	111.2(7)
C(2)−Ru−O(4)	95.6(3)	C(6)−O(6)−Ru	123.1(6)
X(3)−Ru−O(4)	172.0(3)	O(7)−C(6)−O(6)	127.7(9)
O(8)−Ru−O(4)	81.7(2)	O(7)−C(6)−C(7)	119.5(8)
C(1)−Ru−O(6)	93.7(3)	O(6)−C(6)−C(7)	112.7(7)
C(2)−Ru−O(6)	175.5(3)	C(8)−O(8)−Ru	121.1(5)
C(3)−Ru−O(6)	92.8(4)	O(9)−C(8)−O(8)	129.0(9)
O(8)−Ru−O(6)	83.4(2)	O(9)−C(8)−C(9)	120.0(8)
O(4)−Ru−O(6)	81.1(2)	O(8)−C(8)−C(9)	111.0(7)

of $Ru_3(CO)_{12}$ in the presence of carboxylic acids.[2]

$$2Ru_3(CO)_{12} + 6CF_3COOH \longrightarrow 3H_2 + 3Ru_2[\mu\text{-}\eta^2\text{-}OC(CF_3)O]_2(CO)_6 + 6CO \quad (1)$$

1a

$$\rightleftharpoons \begin{matrix} -CO \\ +L \end{matrix}$$

$$3Ru_2[\mu\text{-}\eta^2\text{-}OC(CF_3)O]_2(CO)_4L_2$$

1b

L = H_2O, diglyme

More surprising is the accumulation of the Ru(II) carbonyl **2** during the catalytic process with added CF_3COOCs. On the other hand, the high wavenumbers for the CO stretching vibrations of **2** indicate electrophilic character of the CO ligands as required for the WGSR mandatory intermediate undergoing

Scheme 1. Overall Reactions Resulting in the Acid-Cocatalyzed WGSR Promoted by Ruthenium Carbonyls

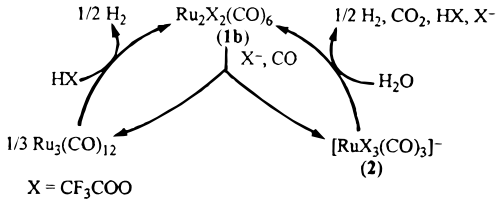

attack by H_2O. An investigation on the origin of **2** and on its reaction with H_2O was then undertaken. As a result, we found that **2** is the product of a hitherto unrecognized disproportionation reaction of **1a**. In anhydrous THF, **1a** is stable under CO, while, under an inert atmosphere, **1b** is unaffected by excess CF_3COO^-. When both these ligands are present, however, gas absorption takes place at room temperature; the disproportionation reaction is pointed out by the formation of orange insoluble $Ru_3(CO)_{12}$, while the characteristic IR absorptions of **2** become evident in the solution. Quantitative recovery of $Ru_3(CO)_{12}$ and **2** as well as gas volumetric measurement of reacted CO, indicate the stoichiometry of eq 2.

$$3Ru_2[\mu\text{-}\eta^2\text{-}OC(CF_3)O]_2(CO)_6 + 3CF_3COO^- + 3CO \xrightarrow{THF} Ru_3(CO)_{12} + 3[fac\text{-}Ru(OCOCF_3)_3(CO)_3]^- \quad (2)$$

1a **2**

The reactions 1 and 2 account for the formation of the intermediates **1a**,**b** and **2**, which were found to accumulate during the catalytic process. Under catalytic conditions, $Ru_3(CO)_{12}$ becomes a labile intermediate. At low CF_3COO^- concentrations, the disproportionation reaction 2 constitutes the slow step of the WGSR; on the other hand, CF_3COO^- together with CO promotes the conversion of **1a** into the more labile **2**, till the enhanced process rate at high CF_3COO^- concentrations is controlled by the reaction consuming **2**, *i.e.* by the reaction with H_2O which produces CO_2 and H_2. As a matter of fact, when **2** was warmed under an inert atmosphere to the same temperature (95 °C) and in the same medium of the catalytic process, H_2 and CO_2 were produced in a 1/2 ratio, together with **1b** which was identified on the basis of its IR spectrum (eq 3).

$$2[fac\text{-}Ru(OCOCF_3)_3(CO)_3]^- + 2H_2O \xrightarrow[\text{inert atmosphere, 95 °C}]{[CF_3COOH] = 0.5\text{ M, 8 M } H_2O\text{ in diglyme}} H_2 + 2CO_2 + Ru_2[\mu\text{-}\eta^2\text{-}OC(CF_3)O]_2(CO)_4L_2 + 2CF_3COO^- + 2CF_3COOH \quad (3)$$

2 **1b**

Reactions 1−3 result altogether in a catalytic cycle (Scheme 1) producing CO_2 and H_2 from CO and H_2O.

Origins and Nature of the Hydrido Intermediates for Dihydrogen Formation. The distinctive aspect of such a WGSR (Scheme 1) is that Ru(0) and a CO ligand in a Ru(II) complex alternate in supplying electrons for dihydrogen formation. Since the knowledge of the ruthenium hydrides which arise from $Ru_3(CO)_{12}$ in acidic media can be of general utility for a better understanding of several catalytic reactions besides WGSR, we devoted a particular effort to identify the hydrido intermediates in the two reductions of the proton respectively in the left- and right-hand branches of Scheme 1.

(a) From $Ru_3(CO)_{12}$ and HX. In the case of H_2 being formed from $Ru_3(CO)_{12}$ and CF_3COOH, it has been shown that the mononuclear hydrido Ru(II) complex $[RuH(OCOCF_3)(CO)_2(py)_2]$ can be trapped when the N-donor ligand pyridine is present.[17] By analogy, we assume that the more labile $RuH(OCOCF_3)(CO)_2L_2$ (L = H_2O or diglyme) (**3b**) is formed *via* oxidative addition of CF_3COOH to $Ru_3(CO)_{12}$ under the conditions of catalysis and constitutes the intermediate for the dihydrogen production of the left-hand branch of Scheme 1. More details on dihydrogen evolution from **3b** are given in section b, since the low-temperature reaction between **2** and H_2O in neutral solution allows this intermediate to be synthesized and, thus, its properties to be separately investigated.

(b) From 2 and H_2O. As mentioned before, reaction 3 between **2** and 8 M H_2O in diglyme requires high temperatures to occur when tested in the same medium of catalysis, *i.e.* in the presence of 0.5 M CF_3COOH. However, in the absence of acid, **2** undergoes nucleophilic attack by H_2O already at room temperature, and hydrido intermediates can be detected under these milder conditions. The addition of water to 0.036 M **2** in diglyme at 20 °C brings about modifications in the IR spectrum of the solution: the absorptions of **2** are replaced by two bands at 2041 and 1957 cm^{-1}, indicative for a *cis*-dicarbonyl complex, and one at 2338 cm^{-1}, this latter being due to the produced CO_2. The reaction is complete in 45 min; no dihydrogen is formed under these conditions, thus suggesting that the production of CO_2 leaves a stable hydrido *cis*-dicarbonyl complex of Ru(II). Any attempt to isolate this species failed, and its nature was ascertained by chemical and spectroscopic methods.

When the reaction between **2** and H_2O was carried out in THF-d_8 ([**2**] = 0.4 M, [H_2O] = 8 M), the ^1H NMR spectrum of the resulting solution showed a hydridic peak at −13.8 ppm, accompanied by two minor resonances at −13.4 and −14.0 ppm (Figure 4a).

By analogy with the recently reported case of the hydridosulfonatocarbonyl(pyridine)ruthenium(II),[17] the three resonances were tentatively attributed to an equilibrium mixture of anionic, neutral, and cationic Ru(II) hydrido dicarbonyl complexes formed by different degrees of substitution of trifluoroacetato by neutral H_2O or THF ligands (eq 4).

$$[fac\text{-}Ru(OCOCF_3)_3(CO)_3]^- + H_2O \xrightarrow{THF} CO_2 + [RuH(OCOCF_3)_2(CO)_2L]^- + CF_3COOH \quad (4)$$

2 **3a**

$$\updownarrow\ -CF_3COO^- + L$$

$$RuH(OCOCF_3)(CO)_2L_2$$

3b

$$\updownarrow\ -CF_3COO^- + L$$

$$[RuH(CO)_2L_3]^+$$

3c

L = THF, H_2O

In order to confirm that, we examined how the CF_3COO^- relative concentration affects the three resonances. The case of $[CF_3COO^-]/[Ru] = 2$ was investigated by reacting with H_2O

(17) Fachinetti, G.; Funaioli, T.; Marchetti, F. *J. Organomet. Chem.* **1995**, *498*, C20.

in ethers {*fac*-Ru(OCOCF$_3$)$_2$(CO)$_3$[(CH$_3$)$_2$CHOH]} (**4**), whose molecular structure is reported in Figure 3.

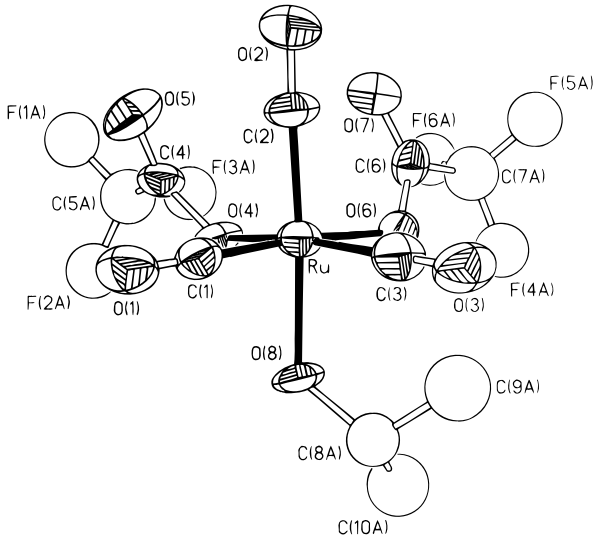

Figure 3. 3. ORTEP projection of the molecular structure of {*fac*-Ru(OCOCF$_3$)$_2$(CO)$_3$[(CH$_3$)$_2$CHOH]} (**4**). Thermal ellipsoids are represented at 30% probability. The disordered CF_3 and $C(CH_3)_2$ groups have been refined with isotropic thermal parameters and are represented by spheres. Moreover, to limit superposition, only one of the two limit positions is shown. The distances and angles around the metal are as follows: Ru−C(2) 1.85(3), Ru−C(1) 1.86(3), Ru−C(3) 1.91(3), Ru−O(4) 2.02(2), Ru−O(6) 2.06(2), Ru−O(8) 2.092(13), C(2)−Ru−C(1) 88.0(12), C(2)−Ru−C(3) 90.9(11), C(1)−Ru−C(3) 91.6(12), C(2)−Ru−O(4) 96.9(9), C(1)−Ru−O(4) 94.4(9), C(3)−Ru−O(4) 170.3(9), C(2)−Ru−O(6) 97.1(10), C(1)−Ru−O(6) 174.7(8), C(3)−Ru−O(6) 89.8(10), O(4)−Ru−O(6) 83.6(6), C(2)−Ru−O(8) 175.6(9), C(1)−Ru−O(8) 90.9(9), C(3)−Ru−O(8) 93.4(9), O(4)−Ru−O(8) 79.0(6), O(6)−Ru−O(8) 83.9(6).

The neutral electrophilic carbonyl complex **4** (ν_{CO} (Nujol): 2153 s, 2094 vs, and 2078 vs cm^{-1}) reacted at room temperature with 8 M H_2O in diglyme at a rate comparable to **2**; the IR spectrum of the solution at the end of the reaction (ν_{CO}: 2041 and 1957 cm^{-1}) shows only minor modifications with respect to that arising from the reaction between **2** and H_2O.

When the reaction between **4** and H_2O is carried out in THF-d_8, however, the ^{1}H NMR spectrum of the resulting solution shows only the two hydridic resonances at −13.4 and −13.8 ppm (Figure 4b), while the third resonance at −14.0 ppm becomes evident only when CF_3COOCs is added to the solution: the three NMR resonances, in a ratio identical to that in Figure 4a from the reaction between **2** and H_2O, are observed when CF_3COOCs is added in equimolar amount with respect to Ru. In a separate experiment we examined the effect of the added strong acid CF_3SO_3H onto the spectrum of Figure 4b. Under the hypothesis that the equilibria in (4) are responsible for the three hydridic resonances, it is expected that the addition of an acid (strong enough to protonate the trifluoroacetate ions released in the solution) results in the accumulation of the cationic species. Accordingly, the addition of increasing amounts of triflic acid enhances the most downfield resonance, as shown in Figure 4c−f. Being that the molar ratio CF_3SO_3H/Ru = 2.40, the two IR bands at 2041 and 1957 cm^{-1} observed at the end of the reaction between **4** (or **2**) and H_2O are shifted to higher frequencies (2047 and 1963 cm^{-1}), as a consequence of the CF_3SO_3H-promoted accumulation of the cationic species. These findings demonstrate the intervention of CF_3COO^- ligands in generating the three hydrido species from **2** and H_2O, and it is likely that the three resonances at −14.0, −13.8, and −13.4 ppm (Figure 4a) are attributable to **3a**, **3b**, and **3c**, respectively. All the three are *cis*-dicarbonyl hydrido complexes; moreover, hydride chemical shifts of less than −10 ppm exclude the presence of CO groups trans to the hydrido ligand.[18] Remarkably, while the neutral **3b** is the dominant species in a neutral solution, the addition of a strong acid to the mixture of hydrido complexes converts **3a** and **3b** into **3c**, a conclusion which will be reviewed again in the next section.

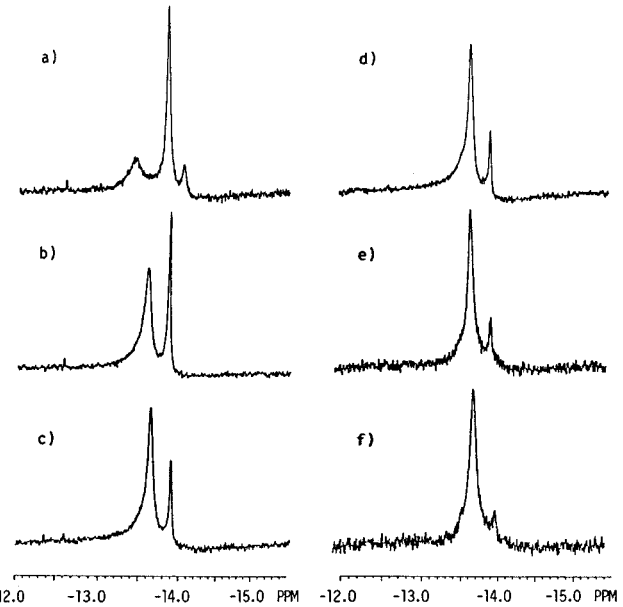

Figure 4. ^{1}H NMR spectra of hydrides accumulating at room temperature in the reaction between Ru(II) carbonyls and H_2O in THF-d_8: (a) Same spectrum obtained directly from **2** or on adding CF_3COOCs to the hydride mixture arising from **4**; (b) spectrum obtained directly from **4**; (c−f) spectra showing the modifications induced on adding increasing amounts of triflic acid to the solution of spectrum b.

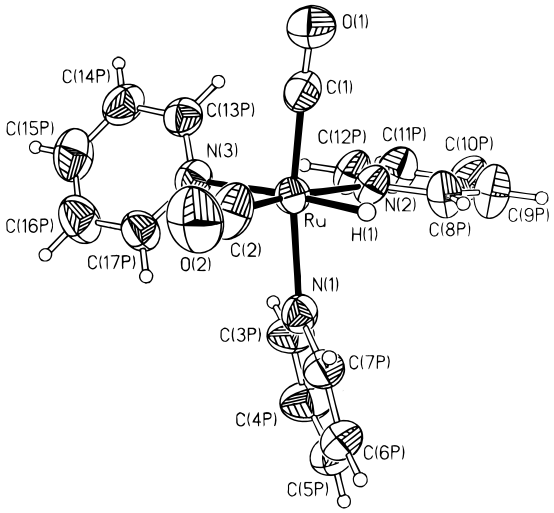

Figure 5. Projection of the cation in the structure of [RuH(CO)$_2$(py)$_3$)][BPh$_4$]. Thermal ellipsoids are represented at 50% probability.

Dihydrogen Formation from 3a−c. As required in the overall reaction 3, dihydrogen production from the mixture of

Finally, the nature of the hydrido complexes arising from the nucleophilic attack of H_2O onto **2** or **4** has been proven by treating their mixture with pyridine, which nearly quantitatively converts **3a−c** into the isolable and structurally characterized hydrido cationic complex [*fac*-RuH(CO)$_2$(py)$_3$]$^+$,[17] whose structure is shown in Figure 5 with the main bond distances and angles in Table 3.

(18) Kaesz, H. D.; Saillant, R. B. *Chem. Rev.* **1972**, *72*, 231.

Table 3. Bond Lengths (Å) and Angles (deg) for the Cation $[RuH(CO)_2(py)_3]^+$

Ru−C(1)	1.850(7)	C(6P)−C(7P)	1.362(9)
Ru−C(2)	1.861(7)	N(2)−C(12P)	1.334(7)
Ru−N(1)	2.149(5)	N(2)−C(8P)	1.339(7)
Ru−N(2)	2.185(5)	C(8P)−C(9P)	1.379(9)
Ru−N(3)	2.284(4)	C(9P)−C(10P)	1.351(9)
Ru−H(1)	1.58[a]	C(10P)−C(11P)	1.379(9)
C(1)−O(1)	1.141(8)	C(11P)−C(12P)	1.369(8)
C(2)−O(2)	1.145(7)	N(3)−C(13P)	1.330(8)
N(1)−C(3P)	1.343(7)	N(3)−C(17P)	1.344(8)
N(1)−C(7P)	1.350(7)	C(13P)−C(14P)	1.387(7)
C(3P)−C(4P)	1.361(9)	C(14P)−C(15P)	1.347(11)
C(4P)−C(5P)	1.361(9)	C(15P)−C(16P)	1.376(11)
C(5P)−C(6P)	1.363(9)	C(16P)−C(17P)	1.380(8)
C(1)−Ru−C(2)	87.2(3)	C(7P)−C(6P)−C(5P)	119.3(6)
C(1)−Ru−N(1)	170.2(2)	N(1)−C(7P)−C(6P)	123.6(6)
C(2)−Ru−N(1)	94.2(3)	C(12P)−N(2)−C(8P)	117.1(5)
C(1)−Ru−N(2)	93.7(2)	C(12P)−N(2)−Ru	124.5(4)
C(2)−Ru−N(2)	171.0(2)	C(8P)−N(2)−Ru	118.5(4)
N(1)−Ru−N(2)	83.4(2)	N(2)−C(8P)−C(9P)	121.9(6)
C(1)−Ru−N(3)	97.5(2)	C(10P)−C(9P)−C(8P)	120.5(6)
(C2)−Ru−N(3)	95.5(2)	C(9P)−C(10P)−C(11P)	118.1(6)
N(1)−Ru−N(3)	92.0(2)	C(12P)−C(11P)−C(10P)	118.8(6)
N(2)−Ru−N(3)	93.3(2)	N(2)−C(12P)−C(11P)	123.6(6)
O(1)−C(1)−Ru	174.5(5)	C(13P)−N(3)−C(17P)	117.3(5)
O(2)−C(2)−Ru	175.2(6)	C(13P)−N(3)−Ru	121.4(4)
C(3P)−N(1)−C(7P)	115.4(5)	C(17P)−N(3)−Ru	120.6(4)
C(3P)−N(1)−Ru	123.0(4)	N(3)−C(13P)−C(14P)	122.8(7)
C(7P)−N(1)−Ru	121.2(4)	C(15P)−C(14P)−C(13P)	119.0(7)
N(1)−C(3P)−C(4P)	123.6(6)	C(14P)−C(15P)−C(16P)	119.8(6)
C(5P)−C(4P)−C(3P)	119.6(6)	C(15P)−C(16P)−C(17P)	118.2(8)
C(4P)−C(5P)−C(6P)	118.4(6)	N(3)−C(17P)−C(16P)	122.9(6)

[a] The H(1) atom coordinates have been refined with constraints.

hydrides **3a**−**c** is expected, and we investigated the required conditions for that. Under an inert atmosphere, 0.05 M **4** was reacted at room temperature with 8 M H_2O in diglyme, till CO_2 production ceased. By the increase of the temperature to 65 °C, dihydrogen evolved from the solution, and the reaction was monitored by determining the H_2/Ru molar ratio at various stages. It can be seen from Figure 6 that its limit value is 0.5, thus indicating the reductive elimination (eq 5), which involves only hydrido ligands and no active hydrogen atoms from the medium.

$$\underset{\mathbf{3b}}{2RuH(OCOCF_3)(CO)_2L_2} \xrightarrow[-2L]{65\ ^\circ C,\ H_2O/diglyme} H_2 + \underset{\mathbf{1b}}{Ru_2[\mu\text{-}\eta^2\text{-}OC(CF_3)O]_2(CO)_4L_2} \quad (5)$$

$$L = H_2O, \text{ diglyme}$$

According to reaction 5, IR absorptions at 2043, 1989, and 1958 cm^{-1} after a long reaction time revealed that **1b** is the product accompanying dihydrogen formation. The intervention of active hydrogen atoms from the medium was excluded even in acidic solution. As mentioned before, rather than giving rise to H_2, CF_3SO_3H converts hydrides **3a**,**b** into the cationic species **3c**, which was found inert toward H_2 formation. As a matter of fact, we observed that at 65 °C dihydrogen production slows down on increasing the amount of added acid (Figure 6). It stops for $[CF_3SO_3H]/[Ru] = 5$; a temperature of 95 °C was then required for restoring slow H_2 production.

On these grounds we exclude that dihydrogen formation in the overall reaction 3 is the result of simple protonation of the hydrido intermediate complexes. More probably, the dihydrogen-eliminating intermediate has the nature of a trifluoroacetato-bridged diruthenium dihydrido complex, whose sulfinate-bridged analog has been fully characterized.[19]

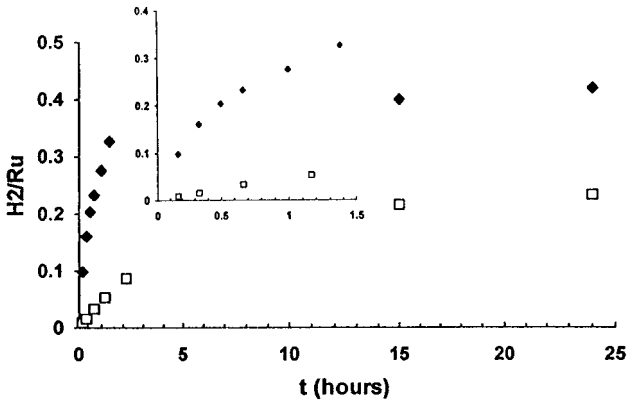

Figure 6. Dihydrogen evolution at 65 °C from the mixture of hydrides **3a**−**c** ([Ru] = 0.05 M). Plots of the H_2/Ru molar ratio *vs* time, with (□) and without (♦) added 0.075 M CF_3SO_3H.

Scheme 2. Fundamental Chemistry of Ruthenium Carbonyls in Acidic Media

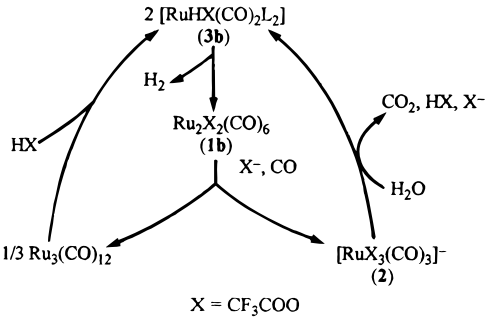

Conclusions. By including the findings on the origin and stability of the hydrido intermediates into the cycle drawn in Scheme 1, we can summarize the chemistry of ruthenium carbonyls in acidic media[20] as in Scheme 2.

The same hydrido intermediate **3b** is formed in two distinct reactions, namely the oxidative addition of the acid to $Ru_3(CO)_{12}$ and the nucleophilic attack by H_2O onto a CO ligand in **2**, followed by CO_2 elimination from the metal hydroxycarbonyl. The role attributed to an acidic cocatalyst for WGSR is generally the protonation of a hydrido intermediate to produce dihydrogen.[21] On the contrary, in the present case H^+ hampers dihydrogen evolution from the mixture of hydrides **3a**−**c** as well as nucleophilic attack by water onto **2**: the only role here recognized for acidity is in the oxidative addition of HX to $Ru_3(CO)_{12}$. On the other hand, the hitherto neglected intervention of the conjugated base is critical in promoting the disproportionation reaction of **1a**, and is required for the formation of the higher oxidation state complex **2**, whose CO ligands can undergo nucleophilic attack by water. The need for a coordinating conjugated base which assists the disproportionation reaction renders the exceptionally strong acid CF_3SO_3H

(19) Siedle, A. R.; Newmark, R. A.; Pignolet, L. H. *Inorg. Chem.* **1986**, *25*, 1345.

(20) The conclusions of the present work are likely to apply also in the case of H_2SO_4, the first employed acidic cocatalyst for the WGSR. In fact, IR absorptions due to dinuclear Ru(I) carbonyl complexes analogous to **1a** or **1b** (ν_{CO}: 2063 m, 2042 s, 2004 m, and 1959 s cm^{-1}) and to a Ru(II) carbonyl complex analogous to **2** (ν_{CO}: 2154 m and 2083 s cm^{-1}) were detected during a catalytic run carried out in diglyme under the following conditions: [Ru] = 0.036 M, [H_2O] = 8 M, [H_2SO_4] = 0.8 M, T = 95 °C, P_{CO} = 0.9 atm.

(21) (a) Ford, P. C.; Ungermann, C.; Landis, V.; Moya, S. A.; Rinker, R. C.; Laine, R. M. *Adv. Chem. Ser.* **1979**, *No. 173*, 81. (b) Laine, R. C.; Crawford, E. J. *J. Mol. Catal.* **1988**, *44*, 357.

unsuitable as a cocatalyst for WGSR, contrary to H_2SO_4, because of the coordinating power of SO_4^{2-}. A similar role for the disproportionation reaction was ascertained also in the acid-cocatalyzed WGSR promoted by rhodium carbonyls in pyridine.[15]

Acknowledgment. This work was supported by the Ministero della Ricerca Scientifica e Tecnologica (MURST). We thank Prof. S. Merlino and Dr. G. Fochi for helpful discussions, Dr. G. Uccello-Barretta for helping in determining an acid dissociation constant, Dr. U. Englert, Aachen University, Aachen, Germany, for intensity data collection on a $[RuH(CO)_2(py)_3][BPh_4]$ single crystal, Mr. F. Del Cima for technical assistence, and Chimet SpA for a gift of ruthenium.

Supporting Information Available: Three X-ray crystallographic files, in CIF format, are available. Access information is given on any current masthead page.

IC960630V